Combined archaeomagnetic and thermoluminescence study of a brick kiln excavated at Fontanetto Po (Vercelli, Northern Italy)

Combined archaeomagnetic and thermoluminescence study of a brick kiln excavated at Fontanetto Po (Vercelli, Northern Italy)

Tema, E.[1,2,*], Fantino, F.[3], Ferrara, E.[4], Lo Giudice, A.[3], Morales, J.[5], Goguitchaichvili, A.[5,6], Camps, P.[7], Barello, F.[8], Gulmini, M.[9]

[1] *Dipartimento di Scienze della Terra, Università degli Studi di Torino, via Valperga 35, 10125, Torino, Italy, evdokia.tema@unito.it*
[2] *ALP-Alpine Laboratory of Palaeomagnetism, via G.U. Luigi Massa 6, 12016, Peveragno, Italy*
[3] *Dipartimento di Fisica, Università degli Studi di Torino and INFN sezione di Torino, via Pietro Giuria 1, 10125 Torino, Italy, fantino@to.infn.it, alessandro.logiudice@unito.it*
[4] *Istituto Nazionale di Ricerca Metrologica, Strada delle Cacce 91, I-10135 Torino, Italy, e.ferrara@inrim.it*
[5] *Laboratorio Interinstitucional de Magnetismo Natural, Instituto de Geofisica, UNAM, Campus Morelia, Michoacan, Mexico, jmorales@geofisica.unam.mx, avto@geofisica.unam.mx*
[6] *Laboratorio de Paleomagnetismo, Departamento de Física, Escuela Politécnica Superior, Universidad de Burgos, C/Francisco de Vitoria, s/n, 09006, Burgos, Spain.*
[7] *Géosciences Montpellier, CNRS and Université Montpellier 2, Montpellier, France, Pierre.Camps@gm.univ-montp2.fr*
[8] *Soprintendenza per i Beni Archeologici del Piemonte e Museo Antichità Egizie, piazza San Giovanni 2 - 10122 Torino, Italy, federico.barello@beniculturali.it*
[9] *Dipartimento di Chimica, Università degli Studi di Torino, via Pietro Giuria 5, 10125 Torino, Italy, monica.gulmini@unito.it*

[*]Corresponding author: Tel.: +39 0116708395; Fax: +39 0116708398; E-mail address: evdokia.tema@unito.it

Abstract

A combined archaeomagnetic and thermoluminescence study was carried out as part of a rescue archaeological excavation on a kiln discovered during the installation of methane gas pipelines beneath a rice field, along the southern border of Fontanetto Po village (Vercelli province, Italy). A total of 23 independent brick samples have been collected, oriented *in situ* using an inclinometer; the use of magnetic and sun compass was not possible due to the existence of metallic tubes beneath the kiln and a plastic cover above it. Standard archaeomagnetic procedures have been used for the determination of the archaeomagnetic inclination and absolute geomagnetic intensity. Stepwise thermal demagnetization shows a very stable characteristic remanent magnetization and the calculated mean inclination of the 23 samples is I = 65.3^{o} with α_{95}= 2.4^{o} and k = 156. Archaeointensity experiments have been performed using the classical Thellier method as modified by Coe, with regular partial thermoremanent magnetization (pTRM) checks. The cooling rate and remanence anisotropy effects upon thermoremanent magnetization (TRM) have been investigated in all the specimens. A total of 19 archaeointensity determinations (at specimen level) that correspond to linear NRM-TRM plots were used for the calculation of the site mean archaeointensity that is 46.4 ± 2.9 μT. Archaeomagnetic dating results show two possible dating intervals for the last 1000 years, calculated at 95 % confidence interval: a first

one from 1511 to 1614 AD, and a second one from 1768 to 1872 AD. Thermoluminescence (TL) study has been also performed on two brick samples from the kiln's internal wall, using conventional laboratory procedures. According to the thermoluminescence results the kiln's last usage lies between 1796 and 1914 AD. This age is in good agreement with the second dating interval obtained by the archaeomagnetic analysis. The combined archaeomagnetic and thermoluminescence results suggest that the last firing of the kiln could have occurred between the end of the 18th century and the beginning of 20th century.

Keywords: Rescue excavation; archaeomagnetism; thermoluminescence dating; kiln; Italy

1. Introduction

Dating of archaeological material is a key issue in the archaeological research as it can significantly contribute to determine the age and duration of the human occupation of a site and define the chronology of cultural and economic development of a certain area. A wide variety of established and newly developed archaeometric techniques can offer valuable dating tools and in some cases different techniques can be applied to the same artefacts. Archaeomagnetic and thermoluminescence dating methods can, under certain conditions, be applied to the same materials, like baked clays (Becker et al., 1994). There are, however, two essential requirements: the degree of ancient heating should have been sufficiently high (400-500 ^{o}C) and the material must have remained undisturbed since cooling down from its last firing.

Archaeomagnetic dating is based on the fact that many archaeological artefacts (e.g., kilns, hearths, bricks, pottery) contain magnetic particles that, when heated at high temperatures and cooled in the presence of the Earth's magnetic field, may acquire a thermal remanent magnetization (TRM) with direction parallel to the direction of the local field and magnitude proportional to the local field Intensity (Eighmy & Sternberg, 1990). The date of the TRM acquisition can thus be determined by comparing the geomagnetic field elements (Declination, *D*, Inclination, *I* and intensity, *F*) obtained from the remanent magnetization measured on the undisturbed archaeological artefacts with reference secular variation (SV) curves that report the chronological geomagnetic field variations within a certain region (Le Goff et al., 2002; Lanos et al., 2005; Pavón-Carrasco et al., 2011).

The accuracy of archaeomagnetic dating depends on several factors such as the suitability of the studied materials as recorders of the Earth's magnetic field, the measurement's uncertainty, the rate of change of the geomagnetic field in the considered period and the availability of a reference SV curve for the given territory. In Europe, well established SV curves are available for several regions, e.g., France (Bucur 1994; Gallet et al. 2002), Bulgaria

(Kovacheva et al., 1998), Hungary (Márton & Ferencz 2006), Germany (Schnepp & Lanos 2005), and the Balkan Peninsula (Tema & Kondopoulou, 2011) while for Italy only a preliminary directional SV curve is available, spanning the last three thousand years (Tema et al., 2006). During the last years, great progress on geomagnetic field modelling at regional scale has been done and nowadays geomagnetic field models, able to represent the past geomagnetic field vector variation in a certain region, are available. These models can provide reference curves for a geographical point (Pavón-Carrasco et al., 2009; 2010) and be used for archaeomagnetic dating (Pavón-Carrasco et al., 2011). However, since the geomagnetic field direction and intensity fluctuate periodically, comparison with the reference curves can yield multiple potential dating intervals over several centuries; in this case, information based on classical archaeological evidences is essential to overcome the multiple dating problem, while comparison with another independent dating technique can confer further reliability to the results (Becker et al., 1994).

Thermoluminescence (TL) is another dating tool frequently used for age determination of archaeological artefacts (Martini & Sibilia, 2001). This technique can be applied exactly at the same materials that can be dated through archaeomagnetism (e.g., kilns, bricks, pottery) and date exactly the same event (last heating of the material). The TL techniques enable the evaluation of the time elapsed since mineral crystallised grains were last exposed to daylight or heated to a few hundred degrees Celsius (for example the heating of the walls of a kiln during its last use). Thermoluminescence dating is based on the principle that during exposure to light or heat the charges trapped in structural defects within the grains of several minerals, such as quartz and feldspar, are released (optically bleached or thermally annealed). Once the grains are sealed from daylight and remain at ordinary environmental temperatures, the charges induced by naturally occurring radioactivity due to decay processes (Preusser et al., 2008) start to accumulate in the structural defects. The quantity of charges trapped can be measured by means of thermoluminescence signal and it is proportional to the time elapsed since last bleaching or annealing. The TL dating requires the measurement of two quantities: P, that is the total accumulated absorbed radiation dose in selected minerals (so-called archaeological dose or Paleodose) measured in Gray (Gy), and D, that is the annual dose due to the natural radioisotope content of the sample and its surrounding environment, expressed in Gy per year. From these two measurements, the TL age can be subsequently calculated from the basic equation: Age = P/D.

This paper presents the combined archaeomagnetic and thermoluminescence study of a brick kiln brought into light during a rescue excavation at Fontanetto Po, Northern Italy. In parallel with archaeomagnetic and TL dating, the heating processes experienced by the bricks of the kiln's wall were studied through measurement of their magnetic properties acquired after

thermal treatments. The archaeomagnetic age of the kiln was obtained using the Matlab archaeomagnetic dating tool proposed by Pavón-Carrasco et al. (2011). This tool is based on the Bayesian approach (Lanos, 2004) and uses the palaeosecular variation curves given by the regional SCHA.DIF.3K model (Pavón-Carrasco et al., 2009) at the kiln's coordinates. The obtained archaeomagnetic dating interval was further restricted after combination with the TL dating results.

2. Archaeological site and sampling

The studied kiln was discovered near to the small village of Fontanetto Po, Vercelli Province, Northern Italy (Fig.1), at the locality called Mulino San Giovanni (45.19^{o} N, 8.19^{o} E). It is a large (combustion chamber dimensions; 6.40 x 4.40 m), rectangular kiln, unearthed during a rescue excavation for the installation of methane gas pipelines, carried out between November 2009 and March 2010. In the vicinity of the sampled kiln, at least three other similar structures have been identified and according to the archaeologists they probably were part of an important workshop for the production of bricks in the area (Barello et al., 2012). According to an initial hypothesis, the use of the workshop could be connected to the need of a large quantity of bricks for the construction of the Fontanetto Po fortified walls, which were probably built immediately after the village's foundation in 1323 AD (Panero, 1988). Another possibility is the use of the bricks to the construction of the San Giovanni mill dated around 1460 AD; both hypothesis suggest that the kiln could have been in use during medieval times but they do not exclude the continuation of its use till more recent times. In fact, no ceramic fragments or other archaeological findings exist to permit a more precise archaeological dating of the kiln's last use. The only available information comes from the size of the kiln's bricks (27x13x7 cm) that excludes any connection with roman times; their size and form is typical of that used during medieval times and conserved up to nowadays (Mannoni & Milanese, 1988).

The metallic methane pipelines already situated at a depth of around one meter below the structure prevented the reliable use of a magnetic compass and the wooden and plastic protection coverage mounted to protect the kiln from adverse weather conditions made impossible the use of sun compass. The archaeomagnetic study was therefore limited to archaeoinclination and archaeointensity determinations. In the laboratory, at least three cylindrical specimens with standard dimensions (diameter = 25.4 mm, height = 22 mm) were drilled from each sample (named with small letters a, b, c; e.g. for sample F1 we prepared specimens F1-a, F1-b, F1-c). For few long specimens it was possible to prepare more sub-specimens, e.g. F1-a1 and F1-a2. Ceramic materials extracted from two bricks have been used for TL dating.

3. Rock magnetic analysis

3.1 Magnetic mineralogy experiments

The magnetic properties of the collected bricks have been investigated in order to identify the main magnetic carries of the samples and investigate their suitability for archaeomagnetic determinations. Isothermal remanent magnetization (IRM) acquisition curves, IRM-back field curves, thermal demagnetization of the IRM components (Lowrie, 1990) and continous thermomagnetic curves have been obtained for representative samples.

The IRM acquisition and back field curves of representative samples were investigated at the ALP Palaeomagnetic laboratory (Peveragno, Italy) using an ASC pulse magnetizer to impart the IRM, applying stepwise increasing magnetic fields up to 2 T, and a JR6 spinner magnetometer (AGICO) to measure the remanent magnetization. Thermomagnetic curves showing the variation of the magnetic moment versus temperature have been measured at INRIM (Torino) with a Vibrating Sample Magnetometer (VSM model: vector 7410 Lakeshore); thermal treatments were carried out in successive 100 °C increasing temperature steps up to 800 °C. Heating was directly applied in the VSM using a thermal-resistance set-up along with a constant field H = 0.1 T applied to the sample.

The temperature dependence of low-field magnetic susceptibility from ambient temperature up to 700 ^{o}C was monitored at the Palaeomagnetic Laboratory of Thessaloniki (Greece) using a Bartington MS2B susceptibility meter in combination with a MS2WF heating unit.

3.2 Rock magnetic results

The IRM acquisition curves show that in most cases saturation is reached at applied fields of 0.1-0.4 T while in few cases samples remain unsaturated after 2 T peak field (see e.g., sample F19, Fig. 3a). The application of a back field after the 2 T peak field acquisition (Fig. 3b) evidences the dominant presence of a magnetic mineral of low remanent coercive force (around 50 mT) such as magnetite or Ti-magnetite in some cases accompanied by a high coercivity mineral, most probably hematite. Stepwise thermal demagnetization of composite IRM (Lowrie, 1990) shows a dominant low- and intermediate- coercivity components removed together with a minor high-coercivity component at temperatures around 460-520 ^{o}C (Fig. 4a). These results confirm that low-Ti magnetite is the main ferromagnetic mineral in the samples, with the presence of minor Ti- hematite content in some samples.

Thermomagnetic curves are useful indicators of the thermal stability of baked materials and consequently of their suitability for archaeomagnetic studies. The heating and cooling curves obtained show good reversibility (Fig. 4b) for most of the samples indicating that no important

mineralogical changes took place during heating up to 600 °C; at higher temperatures, important modification of the ferrimagnetic constituents can occur (see Fig. 5); e.g. the deployment of hematite in the silicate matrix above 800 °C.

The magnetic behavior exhibited during experimentally controlled heating of small brick fragments (mass ~ 20-40 mg) extracted from samples F7, F10, F12, F18, F19, and F22 has been investigated. The samples were subsequently heated and cooled down at room temperature at 100 ^{o}C increasing temperature steps, from 400 ^{o}C up to 900 ^{o}C. All thermomagnetic curves (Fig. 5) show a collapse of magnetization corresponding to the Curie point of magnetite and/or Ti-magnetite (~ 480-520 °C). In few samples (e.g. F22) a second Curie point at temperature around 700 to 750 °C can be observed indicating the presence of some hematite and/or Ti-hematite as already shown by the IRM curves. Samples F7, F10, F19 and F22 show quite stable heating-cooling curves up to temperatures of 500-600 ^{o}C while at higher temperatures important changes in their magnetization are observed. Sample F12 shows quite stable magnetic behaviour also at high temperatures (600 to 800 ^{o}C); on the contrary sample F18 is the less stable one, with a continuously increasing magnetization after each temperature treatment from 400 to 800 ^{o}C. These results suggest that most samples are quite stable at temperatures up to 500 ^{o}C and can be therefore used for archaeointensity determinations for which the thermal stability of the samples is an important factor for successful experiments. Few samples (e.g. F18) that show thermal unstable behaviour during heating may present low success rate during the archaeointensity experiments. The obtained thermal results also show that during the use of the kiln, all samples have experienced temperatures ranging from 500 to 700 ^{o}C, depending on their position in the kiln. Such temperatures are high enough to reset the magnetic remanence and thermoluminesce signals in the past and guarantee reliable results for both archaeomagnetic and TL dating.

4. Archaeomagnetic dating

4.1 Archaeomagnetic inclination: experiments and results

The NRM of the 23 bricks has been measured using a JR-5 spinner magnetometer at the ALP palaeomagnetic laboratory at Peveragno, Italy. Cylinder specimens drilled from the bricks have been stepwise thermally demagnetized up to 580^{o} C using a TSD-2 Schonstedt furnace. Demagnetization diagrams (Fig. 6) show that the magnetic remanence is very stable and it consists of one well defined ChRM component while secondary components, if any, are easily removed at low temperature (< 140^{o}C). The ChRM characteristics point to a primary origin of the thermal remanent magnetization (TRM) acquired during the kiln's last firing.

The inclination of the ChRM for each sample has been obtained from principal component analysis (Zijderveld, 1967; Kirschvink, 1980) and is reported in Table 1. Due to the

missing *in situ* azimuth orientation of the samples, the declination values were not taken in consideration and the mean inclination of the 23 samples has been calculated according to Arason & Levi (2010) and is: I= 65.3^{o}, with uncertainty and precision parameters α_{95}= 2.4^{o} and k= 156, respectively (Table 1).

4.2 Archaeomagnetic intensity: experiments and results

Archaeointensity measurements have been carried out at the LIMNA palaeomagnetic laboratory of UNAM (Campus Morelia, Mexico). The Thellier-Coe type experiments (Thellier & Thellier, 1959; Coe, 1967) were performed with an ASC Scientific TD48-SC furnace; all heating/cooling runs were performed in air. Ten temperature steps were distributed from 250 °C to 540 ºC. The direct laboratory field of 30.0 ± 0.05 μT was applied during heating and cooling along the cylindrical axis (z) of the samples. The magnetic remanence was measured with a JR5 spinner magnetometer. Regular partial thermoremanent magnetization (pTRM) checks were done at every three temperature steps together with additional pTRM tail checks (Riisager and Riisager, 2001) performed at two intermediate temperatures (350 ºC and 450 ºC).

Estimations of the original cooling time in this type of kilns, from the highest temperature (probably around 700 ºC) to ambient temperature are around 6 to 10 hours, whereas average cooling time in laboratory (using a TD48 thermal demagnetizer with fan on) ranges from 30 to 45 min; this means a difference of one order of magnitude between the natural and experimental cooling rate. According to experimental results on synthetic SD-type particles, this difference may produce an archaeointensity overestimation up to 7 percent (Fox and Aitken, 1980; McClellen-Brown, 1984). Very few studies are devoted to the cooling rate effect on the TRM acquisition by pseudo-single-domain (PSD) grains – the most abundant magnetic grain size typology of materials in rocks and burned archeological artifacts. It is therefore evident the need of cooling rate corrections on raw Thellier-type intensities. The cooling rate dependence of TRM was here investigated following a modified procedure to that described by Chauvin et al., (2000) (see Morales et al., 2009), using a slow cooling time of 6 h from 540 ºC to 20 ºC.

Measurements of the TRM anisotropy (ATRM) have been carried out at the palaeomagnetic laboratory of Géosciences Montpellier (France), by inducing in the sample a pTRM from 540°C to room temperature along six directions (i.e. +x, +y, +z, −x, −y, −z) with a magnetic field of 50 μT. Zero-field thermal demagnetizations at 560°C before each pTRM acquisition were used as a baseline. TRM tensors were measured on the same specimens used for archaeointensity determination after the last heating step. The TRM anisotropy tensor and the relative anisotropy factors for TRM anisotropy correction were then calculated following the Veitch et al. (1984)'s protocol.

Archaeointensity data were interpreted using NRM-TRM plots (Arai plots, Fig. 7). In order to be considered as reliable estimations of the ancient field, archaeointensity determinations obtained in this study have to fulfill several acceptance criteria (Morales et al., 2009):

1) Directions of natural remanent magnetization (NRM) end-points at each step obtained from archaeointensity experiments have to fall along a straight line, trending toward the origin in the interval chosen for archaeointensity determination.

2) No significant deviation of NRM directions towards the applied field direction should be observed, as revealed in vector (Zijderveld) plots.

3) A number of aligned points (N) on the NRM-pTRM diagram ≥ 5; specimens suspected to carry viscous remanent magnetization acquired *in situ* are rejected.

4) NRM fraction factor (f, Coe et al., 1978) ≥ 0.3. This means that at least 30 per cent of the initial NRM was used for archaeointensity determination (in most of our samples f >0.5).

5) A quality factor $q = (f*g)/ \beta$ (Coe et al., 1978) ≥ 5 (generally above 10, Table 2); g is the gap factor (Coe et al., 1978) and β the relative standard deviation of the slope.

6) Archeointensity results obtained from NRM-pTRM diagrams must not show an evident concave up shape, since in such cases remanence is probably associated with the presence of MD grains (Levi, 1977; Kosterov et al. 1998).

7) Positive pTRM checks, i.e., the deviation of 'pTRM' checks should be less than 15%.

Evaluation of pTRM-tail checks performed at two different temperatures was in most cases lower than 20 %. Seven out of 22 specimens show tail remanences at 350 °C higher than this cut off value, up to 45 %. We note that MD grains may show pTRM-tails as large as 50% (Dunlop and Özdemir, 2000). At 475°C, however, only three specimens retain tail remanences above this critical value.

Cooling rate corrections were applied to all specimens, whose the corresponding change in TRM acquisition capacity was below 15% (Chauvin et al, 2000). The cooling rate procedure followed (Morales at al., 2011) provided for most of the samples cooling rate correction factors (f_{CR}) between 0.988 and 1.140, which corresponds to an overall decrease of the raw intensity values by 7% on average. In few samples the cooling rate correction factors were negative, $f_{CR} < 0$; in these cases no correction was applied (Table 2). The kiln's mean archaeointensity is 46.4 ± 2.9 μT, and was calculated from 19 specimen results (13 independent samples), after the correction of the ATRM and cooling rate effects, when necessary (Table 2).

4.3 Archaeomagnetic dating results

The mean inclination and intensity values obtained for Fontanetto Po kiln have been used for the archaeomagnetic dating of the kiln after comparison with the reference secular variation curves calculated from the SCHA.DIF.3K model (Pavón-Carrasco et al., 2009). The SCHA.DIF.3K is a regional archaeomagnetic model that represents the geomagnetic field variations in Europe for the last 3000 years modelling together the three geomagnetic field elements. It is based on reference data coming from instrumental measurements for the last 400 years and on data from archaeological material for older times. The SCHA.DIF.3K model predicts the geomagnetic field at the site of interest, avoiding this way any eventual relocation error. It also has the advantage that it can provide well-constrained palaeosecular variation curves for regions with poor coverage of archaeomagnetic data, such as Italy (Tema, 2011).

Archaeomagnetic dating of the Fontanetto Po kiln has been carried out using the Matlab *archaeo_dating* tool (Pavón-Carrasco et al., 2011). Inclination and intensity reference curves have been directly calculated at the geographic coordinates of Fontanetto Po and have been used for the calculation of probability density functions separately for site mean inclination and intensity values. The final dating of the kiln is obtained after the combination of the separate density functions for inclination and intensity (Fig. 8). Two possible dating intervals result for the last 1000 years calculated at 95 % confidence interval: a first one from 1511 to 1614 AD, and a second one from 1768 to 1872 AD.

5. Thermoluminescence dating

Thermoluminescence (TL) dating has been carried out at the Physics Department (University of Torino). Two bricks from the internal kiln wall (samples F18 and F19; Fig. 1) have been studied applying the fine grains method (Aitken, 1985). Due to the position of the analysed bricks, the calculated thermoluminescence age is related to the kiln's last use.

5.1 Archaeological Dose evaluation

The archaeological dose or paleodose (P) is the sum of two terms: the equivalent dose (ED) and the supralinearity (I), a phenomenon that occurs at low irradiation doses, i.e., at the initial history of the sample after its fabrication (Aitken, 1985). In order to evaluate the archaeological dose, about two grams of clay have been extracted from each brick avoiding surface material. The chemical procedure described by Vieillevigne et al. (2007) was applied for sample preparation. The equivalent dose, *ED*, was determined using the additive dose method for

multiple aliquots (Fleming, 1970); a calibrated radioactive Sr-90 beta source was used to supply the artificial dose. After irradiation, a pre-heating was performed in oven at 150 ^{o}C for 120 seconds to reduce the contribution to the TL signal coming from unstable traps. All thermoluminescence measurements were carried out by means of a TL2000-Ipses reader in nitrogen atmosphere using a 10 ^{o}C/s heating rate. The measured TL glow curves for sample F19 are shown in Fig. 9. By means of the plateau test, the range 280°C-320°C was identified for integration and comparison of TL signals between natural and irradiated samples. In Fig. 10 the results and the linear fit for the ED calculation are shown.

In order to measure the supralinearity, a second glow analysis at low artificial irradiation doses was carried out after removing natural TL by means of a four-hour 450°C heating in oven (Aitken 1985).

Finally, the anomalous fading was also estimated. Sample aliquots were irradiated with 12 Gys and stored in dark at room temperature for 2 month with other aliquots not irradiated. Then the aliquots not irradiated were exposed to the same dose and the TL signals compared with aliquots irradiated 2 month before. For the samples under investigation no anomalous fading was detected. All the results on ED, I and archaeological dose for F18 and F19 are shown in Table 3.

5.2 Annual Dose evaluation

The annual dose can be calculated as the sum of contributions to the dose from alpha, beta and gamma particles generated during radioactive decays. About one gram of untreated clay from each brick was employed to perform alpha decay counting by means of CALPH-Ipses apparatus. The measured radioactive activity was utilized to calculate the annual dose due to alpha particles supposing an equal contribution to the activity from uranium and thorium decay chains and applying the correction factor k (Table 3). The k-factor that depends on the material, is the efficiency of the alpha particles compared to beta particles in producing a TL signal. It was calculated comparing the measured ED values obtained respectively by means of alpha (Am-241 in vacuum) and beta particle artificial irradiations.

The measured alpha particle activity was also utilized to calculate the annual dose due to beta particles from uranium and thorium decay chains. The beta contribution to annual dose from potassium was calculated after measuring its contents by means of ICP (Ion Coupled Plasma). Since it was not possible to carry out measurements of environmental dose *in situ*, gamma ray contribution to the annual dose was estimated by means of gamma counting (HPGe-ORTEC detection system). Gamma ray measurements were carried out on clay and on excavated soil. In fact, as a first approximation and taking in account the position of the samples F18 and F19 (Fig. 2), it was assumed that gamma ray contribution to annual dose from the environment was given

by the kiln bricks for half of the entire solid angle and to the soil for the remaining. A value of 1.34±0.35 mGy/years was estimated.

Finally, the annual dose contributions were corrected for the bricks porosity; the environmental moisture was arbitrary considerate F=80 ± 20% (Aitken 1985). All the results on annual dose are summarized in Tab. 3.

5.3 Thermoluminesce dating results

On the basis of archaeological dose and annual dose the age of the last heating of the bricks was calculated. There is a good agreement between the values obtained for the two samples. Sample F18 is dated at 1864 AD ± 25 and sample F19 at 1854 AD ± 29 (Table 3). At 95% confidence interval, the proposed thermoluminescence dating of the last firing of the kiln is 1796-1914 AD. This age is in very good agreement with the second dating interval obtained by the archaeomagnetic analysis.

6. Conclusions

Archaeomagnetic study on 23 independent brick samples from the Fontanetto Po kiln yielded very well defined archaeoinclination and archeaointensity values. These values were compared with the reference curves produced by the SCHA.DIF.3K European regional geomagnetic field model and two possible dating intervals were proposed: a first one from 1511 to 1614 AD, and a second one from 1768 to 1872 AD. Further refinement of this dating was offered by the thermoluminescence study on two bricks collected from the internal kiln's wall that resulted in an age between 1796 to 1914 AD. This age is in excellent agreement with the second dating interval obtained by the archaeomagnetic analysis and the combined archaeomagnetic and thermoluminescence results suggest that the last firing of the kiln has probably occurred between the end of the 18th century and the beginning of the 20th century AD. This dating does not contradict the hypothesis of the archaeologists that the kiln was constructed during medieval times but it suggests that the kiln continued to be in use till recent time. The results of this study show that the archaeomagnetic and TL dating techniques can be successfully combined and they can offer a powerful tool for precise dating of backed archaeological artefacts. Their main advantage is that they can be applied at exactly the same material and both methods date exactly the same event (the last firing of the archaeological material). Moreover, thanks to the independent dating information offered by the TL, the obtained archaeoinclination and archaeointensity values can be used as reference points in the secular variation curves and can improve our knowledge about the geomagnetic field's variations in the past. This is particularly important for older time periods for which the only source of information about the

Earth's magnetic field variation is the archaeomagnetic results of well dated archaeological artefacts and/or lava flows.

Acknowledgements

The authors warmly thank Dr. Alessandro Re (National Institute of Nuclear Physics) for his help in thermoluminescence measurements and data analysis. Evdokia Tema acknowledges the Palaeomagnetic laboratory of Thessaloniki for hospitality during the performance of the thermomagnetic experiments. Dr. Javier Pavón-Carrasco and an anonymous reviewer are highly acknowledged for their useful comments on the manuscript.

REFERENCES

Aitken, M.J., 1985. *Thermoluminescence Dating*, Academic Press, London

Arason, P. & Levi, S., 2010. Maximum likelihood solution for inclination-only data in palaeomagnetism. *Geophysical Journal International*, 182, 753-771, doi: 10.1111/j.1365-246X.2010.04671.x

Barello, F., Ferrara, E., Gatti, S., Tema, E., 2012. Fontanetto Po, strada vicinale antica Torino-Casale. Fornaci di epoca moderna e strada glareata romana. *Quaderni della Soprintendenza Archeologica del Piemonte*, 27, 242-244.

Becker, H., Göksu, H.Y., Regulla, D.F., 1994. Combination of archaeomagnetism and thermoluminescence for precision dating. *Quaternary Geochronology (Quaternary Science Reviews)*, 13, 563-567.

Bucur, I., 1994. The direction of the terrestrial magnetic field in France during the last 21 centuries. *Phys. Earth Planet. Inter*., 87, 95-109.

Chauvin, A., Garcia, A., Lanos, Ph., & Laubenheimer, F., 2000. Paleointensity of the geomagnetic field recovered on archaeomagnetic sites from France. *Physics of the Earth and Planetary Interiors,* 120, 111-136.

Coe, R. S., 1967. Paleo-intensities of the Earth's magnetic field determined from Tertiary and Quaternary rocks. *J. Geophys. Res.*, 72 (12), 3247-3262.

Coe, R. S., Grommé, S., Mankinen, E. A., 1978. Geomagnetic paleointensities from radiocarbon-dated lava flows on Hawaii and the question of the Pacific nondipole low. *J. Geophys. Res.*, 83 (B4), 1740-1756.

Dunlop, D.J., Özdemir, Ö., 2000. Effect of grain size and domain state on thermal demagnetization tails. *Geophysical Research Letters*, 27, 1311–1314.

Eighmy, J.L., Sternberg, R.S., 1990. *Archaeomagnetic dating*. Arizona University Press, Tucson, pp. 450.

Fleming S.J., 1970. Thermoluminescence dating: refinement of the quartz inclusion method. *Archaeometry*, 12, 133-143.

Fox, J. M. W., & Aitken, M. J., 1980. Cooling rate dependence of the thermoremanent magnetization. *Nature*, 283, 462-463.

Gallet, Y., Genevey, A. & Le Goff, M., 2002. Three millennia of directional variation of the Earth's magnetic field in Western Europe as revealed by archaeological artefacts. *Phys. Earth Planet. Inter.*, 131, 81-89.

Kirschvink, J.L., 1980. The least-square line and plane and the analysis of palaeomagnetic data. *Geophys. J. Astron. Soc.*, 62, 699-718.

Kosterov, A. A., Perrin, M., Glen, J. M., & Coe, R. S., 1998. Paleointensity of the Earth's magnetic field in Early Cretaceous time: The Parana Basalt, Brazil. *Journal of Geophysical Research*, 103, 9739–9753.

Kovacheva, M., Jordanova, N. & Karloukovski, V., 1998. Geomagnetic field variations as determined from Bulgarian archaeomagnetic data. Part II: The last 8000 years. *Surv. Geophys.*, 19, 431-460.

Lanos, Ph., 2004. Bayesian inference of calibration curves: application to archaeomagnetism. In *Tools for Constructing Chronologies, Crossing Disciplinary Boundaries,* (eds.) Buck, C.E. & Millard, A.R., Series: Lecture Notes in Statistics, Springer-Verlag, London, vol. 177, pp. 43-82.

Lanos, Ph., Le Goff, M., Kovacheva, M. & Schnepp, E., 2005. Hierarchical modelling of archaeomagnetic data and curve estimation by moving average technique. *Geophys. J. Int*., 160, 440-476.

Le Goff, M., Gallet, Y., Genevey, A.,Warmé, N., 2002. On archaeomagnetic secular variation curves and archeomagnetic dating. *Phys. Earth Planet. Int.,* 134, 203-211.

Levi, S., 1977. The effect of magnetite particle size on paleointensity determinations of the Geomagnetic Field. *Phys. Earth Plane. Int.*, 13, 245-259.

Lowrie, W., 1990. Identification of ferromagnetic minerals in a rock by coercivity and unblocking temperature properties. *Geophys. Res. Lett.*, 17, 159-162.

Mannoni, T. & Milanese, M., 1988. Mensiocronologia. In: (Eds) Francovich, R., Parenti, R.: *Archeologia e restauro dei monumenti (I Ciclo di Lezioni sulla Ricerca applicata in Archeologia, Certosa di Pontignano, 1987).* All'insegna del Giglio, Firenze 1988, pp. 383-402.

Martini, M. & Sibilia, E., 2001. Radiation in archaeometry: archaeological dating. *Radiation Physics and Chemistry*, 61, 241-246.

Márton, P. & Ferencz, E., 2006. Hierarchical versus stratification statistical analysis of archaeomagnetic directions: the secular variation curve for Hungary. *Geophys. J. Int.*, 164, 484-489, doi: 10.1111/j.1365-246X.2006.02873.x

McClelland-Brown, E., 1984. Experiments on TRM intensity dependence on cooling rate. *Geophysical Research Letters,* 11, No. 3, 205-208.

Morales, J., Goguitchaichvili, A., Aguilar-Reyes, B., Pineda-Duran, M., Camps, P., Carvallo, C., Calvo-Rathert, M., 2011. Are ceramics and bricks reliable absolute geomagnetic intensity carriers? *Phys. Earth Planet. Int.*, 187, 310-321, doi: 10.1016/j.pepi.2011.06.007.

Morales, J., Goguitchaichvili, A., Acosta, G., González-Morán, T., Alva-Valdivia, L., Robles-Camacho, J., & Hernández-Bernal, M. S., 2009. Magnetic properties and archeointensity determination on Pre-Columbian pottery from Chiapas, Mesoamerica. *Earth Planets & Space*, doi:10.19EPS2364.10.29.

Panero, F., 1988. *Comuni e borghi franchi nel Piemonte medievale.* CLUEB, Bologna, 120-132.

Pavón-Carrasco, F. J., Osete, M.L., Torta, J. M., Gaya-Piqué, L. R., 2009. A regional archaeomagnetic model for Europe for the last 3000 years, SCHA.DIF.3K: applications to archaeomagnetic dating. *Geochem. Geophys. Geosyst.,* 10 (3), Q03013, doi:10.1029/2008GC002244.

Pavón-Carrasco, F. J., Osete, M.L., Torta, J., 2010. Regional modeling of the geomagnetic field in Europe from 6000 BC to 1000 BC. *Geochem. Geophys. Geosyst*, 11, Q11008, doi: 10.1029/2010GC003197.

Pavón-Carrasco, F. J., Rodriguez-Gonzalez, J., Osete, M.L., Torta, J., 2011. A Matlab tool for archaeomagnetic dating. *J. Arch. Sci.*, 38 (2), 408-419.

Preusser, F., Degering, D., Fuchs, M., Hilgers, A., Kadereit, A., Klasen, N., Krbetschek, M., Richter, D., Spencer, J., 2008. Luminescence dating: basics, methods and applications. *Quaternary Science Journal*, 57, 1-2, 95-149.

Riisager, P. & Riisager, J., 2001. Detecting multidomain magnetic grains in Thellier palaeointensity experiments. *Phys. Earth Planet. Int.*, 125, 111–117.

Schnepp, E. & Lanos Ph., 2005. Archaeomagnetic secular variation in Germany during the past 2500 years. *Geophys. J. Int.,* 163, 479-490.

Selkin, P.A. & Tauxe, L., 2000. Long-term variations in palaeointensity. *Philos. Trans. R. Soc. Lond.,* A 358, 1065-1088.

Tema, E., 2011. Archaeomagnetic Research in Italy: Recent achievements and future perspectives. In: *The Earth's Magnetic Interior. (*Eds.): Petrovsky, E., Herrero-Bervera, E.,

Harinarayana, T., Ivers, D., IAGA Special Sopron Book Series, Volume 1, Chapter 15, pp. 213-233, Springer, doi: 10.1007/978-94-007-0323-0_15.

Tema, E., Hedley, I., Lanos, Ph., 2006. Archaeomagnetism in Italy: A compilation of data including new results and a preliminary Italian secular variation curve. *Geophys. J. Int.*, 167, 1160-1171.

Tema, E. & Kondopoulou, D., 2011. Secular variation of the Earth's magnetic field in the Balkan region during the last 8 millennia based on archaeomagnetic data. *Geophys. J. Int.*, *186, 603-614.*

Thellier, E. & Thellier, O., 1959. Sur l'intensité du champ magnétique terrestre dans le passé historique et géologique, *Ann. Geophys.,* 15, 285-376.

Veitch, R.J., Hedley, I.G., Wagner, J.J., 1984. An investigation of the intensity of the geomagnetic field during Roman times using magnetically anisotropic bricks and tiles. *Arch. Sci*. (Geneva) 37 (3), 359–373.

Vieillevigne, E., Guibert, P., Bechtel, F., 2007. Luminescence chronology of the medieval citadel of Termez, Uzbekistan: TL dating of bricks masonries. *J. Arch. Science,* 34, 1402-1416.

Zijderveld, J., 1967. AC demagnetization of rocks: analysis of results. In: Collinson, D., Creer, K., Runcorn, S. (Eds.), *Methods in Paleomagnetism*. Elsevier, New York, pp. 254-256.

Figure captions

Fig. 1. Location of the Fontanetto Po kiln (45.19^{o} N, 8.19^{o} E).

Fig. 2. Studied kiln and position of the samples.

Fig. 3. a) IRM acquisition and b) IRM back-field curves of selected samples.

Fig. 4. a) Stepwise thermal demagnetization of three IRM components for representative samples. Symbols: square = Soft- (0.1 T); triangle = Medium- (0.5 T); diamond = Hard- (1.5 T) coercivity component; b) Representative continuous magnetic susceptibility versus temperature curves.

Fig. 5. Magnetization versus temperature measured using a VSM, for samples F7, F10, F12, F18, F19, and F22. Continuous thermo-magnetic curves obtained during heating and cooling the samples in the VSM.

Fig. 6. Representative Zijderveld diagrams from stepwise thermal demagnetization (open dots = apparent inclination).

Fig. 7. Examples of NRM-TRM plots and associated Zijderveld diagrams from successful (a and b) and rejected (c) archaeointensity experiments.

Fig. 8. Archaeomagnetic dating results obtained using the matlab *archaeo_dating* tool (Pavón-Carrasco et al., 2011). a) Up: inclination reference secular variation curve calculated from the SCHA.DIF.3K model (red curve with error band) and the kiln's measured inclination (blue line with green error band), down: calculated probability density function for inclination; b) Up: intensity reference secular variation curve calculated from the SCHA.DIF.3K model (red curve with error band) and the kiln's measured archaeointensity (blue line with green error band), down: calculated probability density function for intensity; c) combined probability density function for inclination and intensity.

Fig. 9. Measured TL glow curves for sample F19. Beta irradiations were performed in the range 4 Gy – 12 Gy. For each irradiation two samples were prepared and measured.

Fig. 10. Linear fit for Equivalent Dose (ED) calculation.

Table captions

Table 1. Archaeomagnetic inclination results for Fontanetto Po kiln.
Columns: Sample; Temperature interval used for the calculation of the characteristic inclination (I_{ChRM}) at specimen level; Calculated inclination (I) at specimen level; I_{ChRM}= kiln's mean inclination; α_{95}= 95% semi-angle of confidence; k= precision parameter; N= number of samples; n= number of specimens. The kiln's mean value was calculated according to Arason & Levi (2010).

Table 2. Archaeointensity results at specimen level.
Columns: Specimen; Palaeointensity in μT before any correction; Palaeointensity in μT after TRM anisotropy correction; Palaeointensity in μT after ATRM and cooling rate correction (at the specimens indicated with * no cooling rate correction has been applied because of cooling rate factor CR <0); σ: standard deviation in μT; Tmin, Tmax: minimum and maximum temperatures used for the intensity determination; N: the number of heating steps used for the intensity determination; slope: slope of the best fit; β: ratio of the standard error of the slope to the absolute value of the best-fit slope for the data on the NRM-TRM diagram; f, the fraction of NRM used for intensity determination; g: the gap factor; q: the quality factor as defined by Coe et al. (1978); MAD: Maximum angular deviation, DRAT: difference ratio as defined by Selkin and Tauxe (2000); N/R: no result; *Specimens in italics were rejected and therefore not used for the calculation of the site mean.*

Table 3. Summary of the thermoluminescence dating results. No anomalous fading was recognized on F18 and F19 samples and the plateau test was successful in the range 280-320 °C. Gamma dose was estimated by means of gamma ray measurements on clay and on excavated soil.

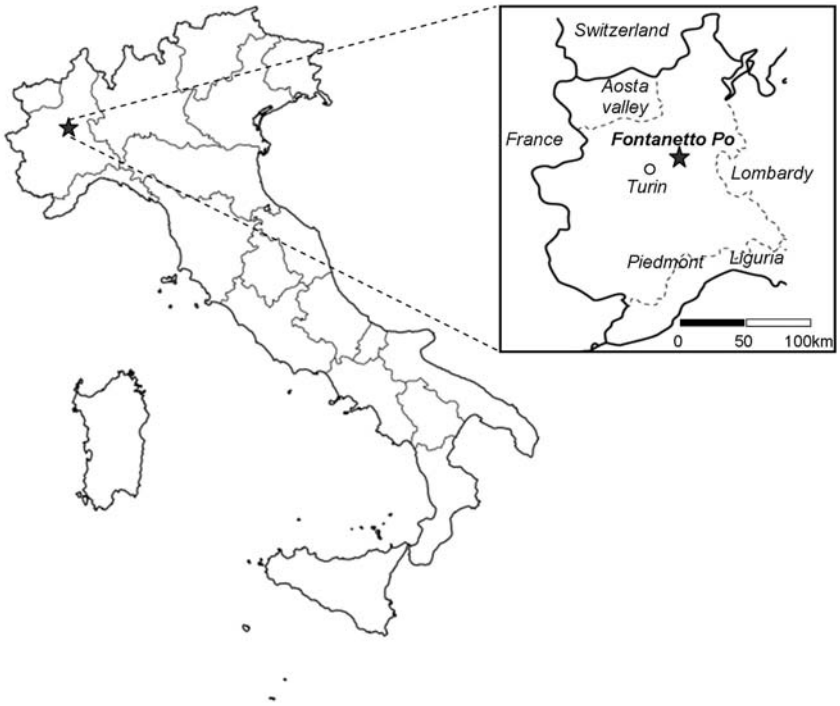
Switzerland
Aosta valley
France
Fontanetto Po
Turin
Lombardy
Piedmont
Liguria
0
50
100km

Fig. 1

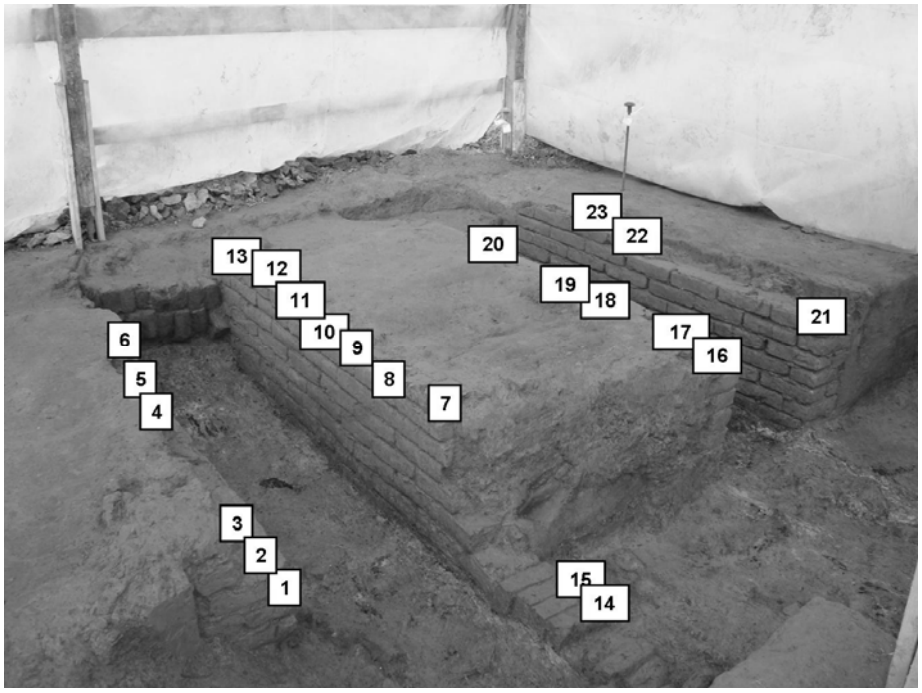

Fig. 2

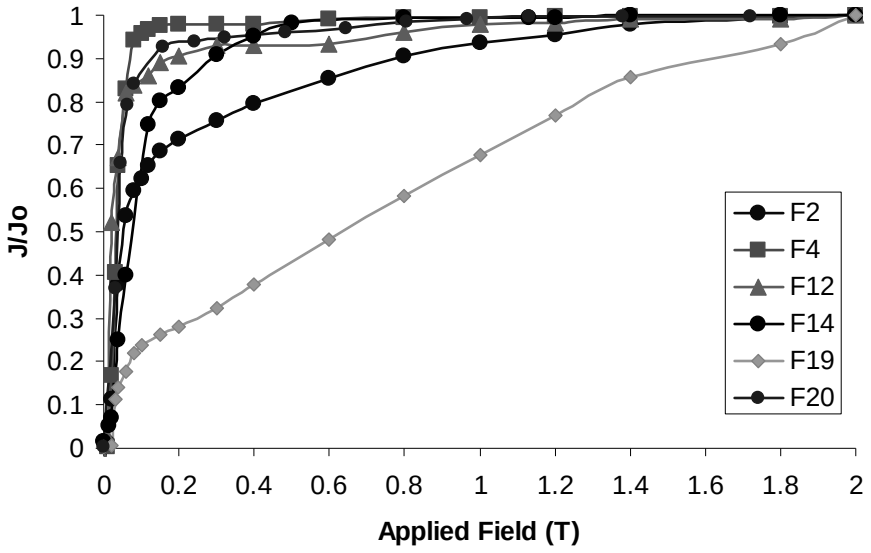

(a)

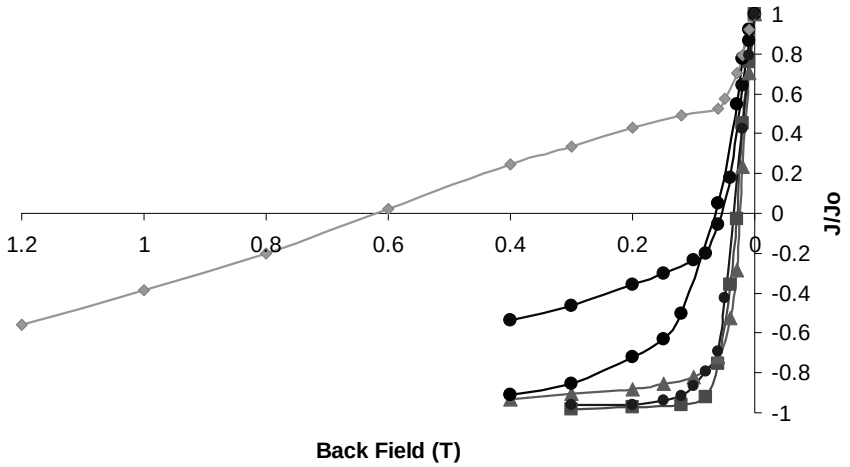

(b)

Fig. 3

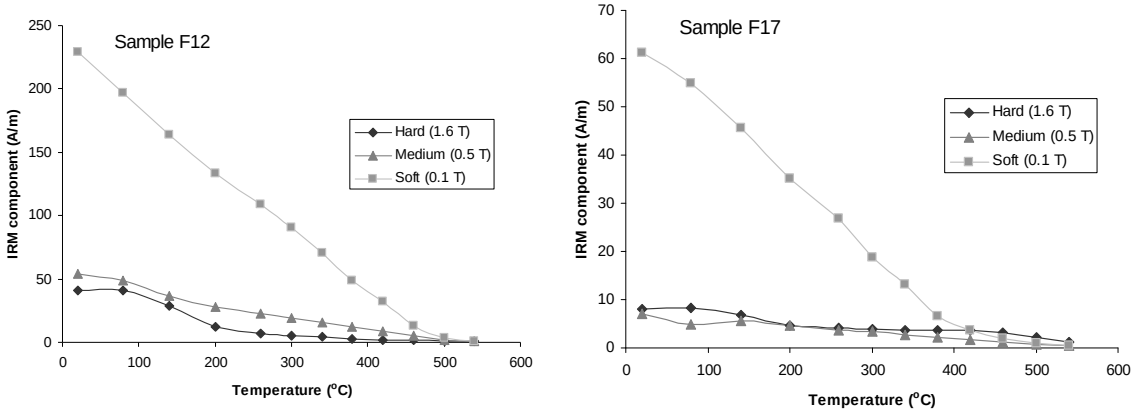
Sample F12
IRM component (A/m)
Temperature (°C)
Hard (1.6 T)
Medium (0.5 T)
Soft (0.1 T)
Sample F17
IRM component (A/m)
Temperature (°C)
Hard (1.6 T)
Medium (0.5 T)
Soft (0.1 T)

(a)

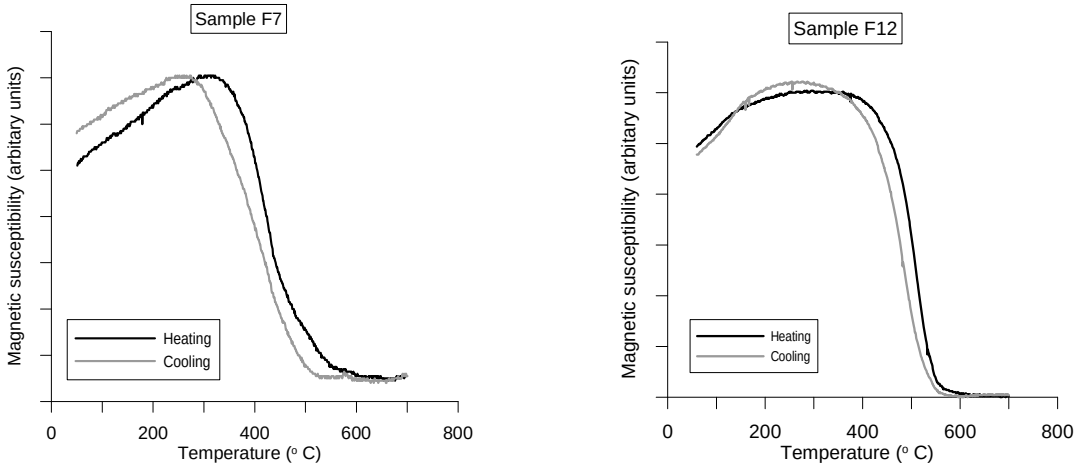
Sample F7
Magnetic susceptibility (arbitary units)
Heating
Cooling
Temperature (° C)
Sample F12
Magnetic susceptibility (arbitary units)
Heating
Cooling
Temperature (° C)

(b)

Fig. 4

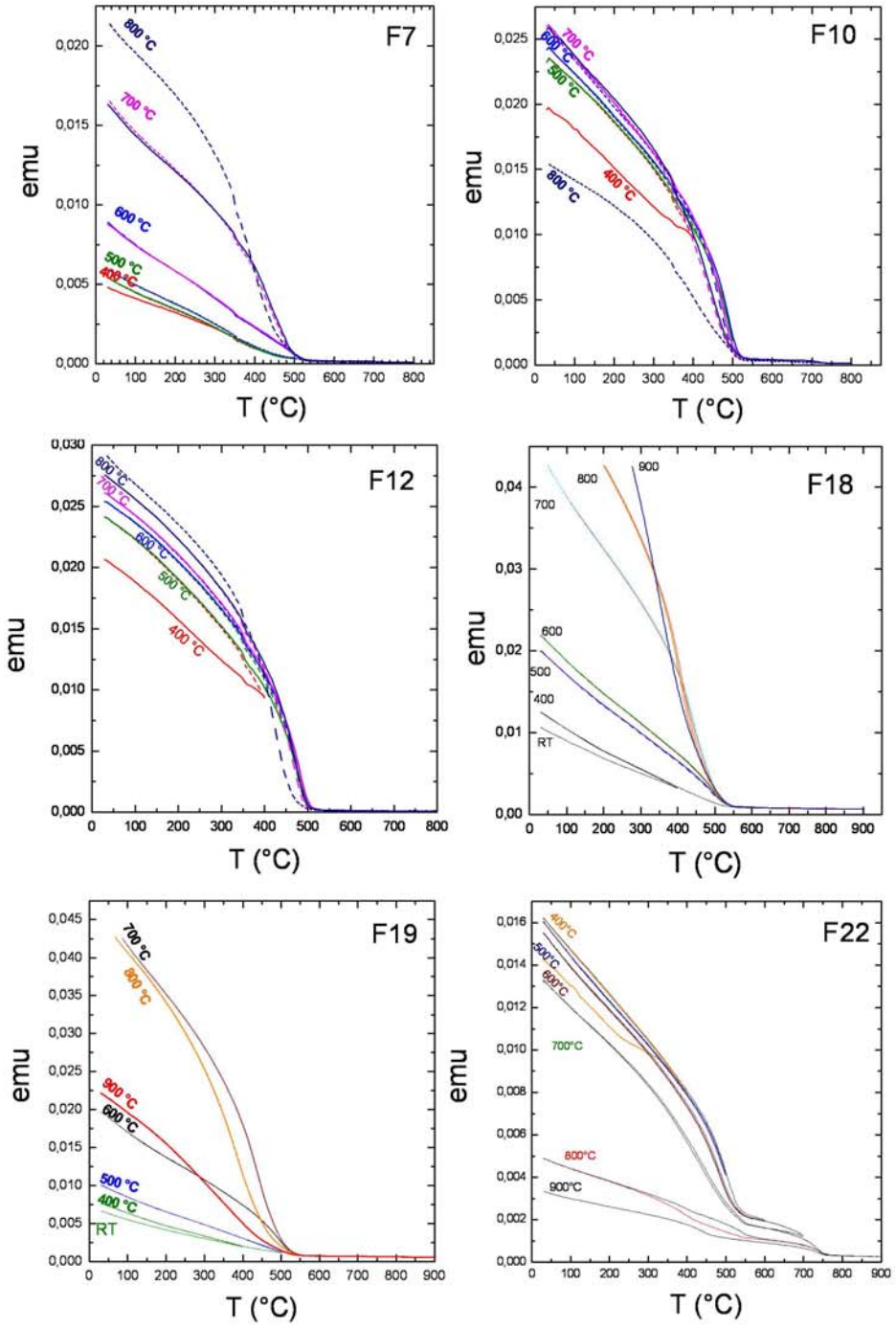
F7
800 °C
700 °C
600 °C
500 °C
400 °C
emu
T (°C)
F10
700 °C
600 °C
500 °C
400 °C
800 °C
emu
T (°C)
F12
800 °C
700 °C
600 °C
500 °C
400 °C
emu
T (°C)
F18
800
900
700
600
500
400
RT
emu
T (°C)
F19
700 °C
800 °C
900 °C
600 °C
500 °C
400 °C
RT
emu
T (°C)
F22
400°C
500°C
600°C
700°C
800°C
900°C
emu
T (°C)

Fig. 5

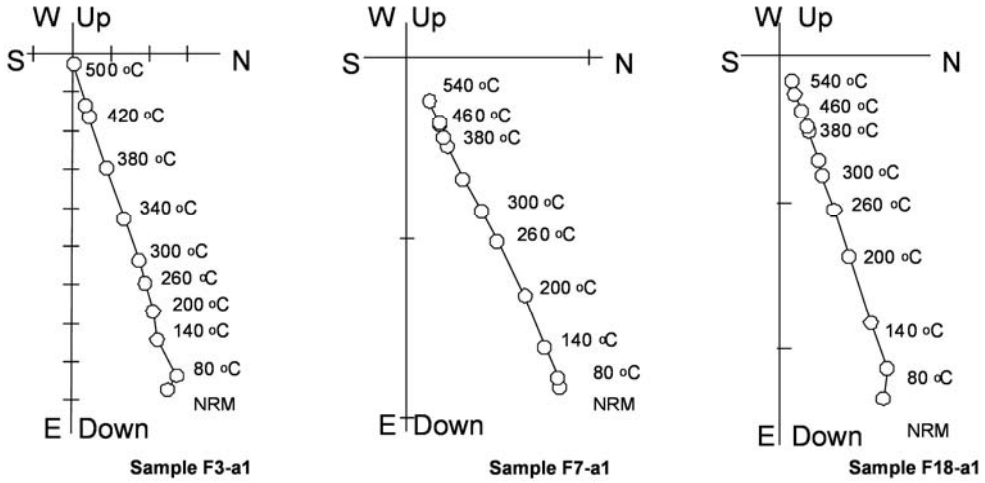
W Up
S
N
E Down
500 oC
420 oC
380 oC
340 oC
300 oC
260 oC
200 oC
140 oC
80 oC
NRM
Sample F3-a1
W Up
S
N
E Down
540 oC
460 oC
380 oC
300 oC
260 oC
200 oC
140 oC
80 oC
NRM
Sample F7-a1
W Up
S
N
E Down
540 oC
460 oC
380 oC
300 oC
260 oC
200 oC
140 oC
80 oC
NRM
Sample F18-a1

Fig. 6

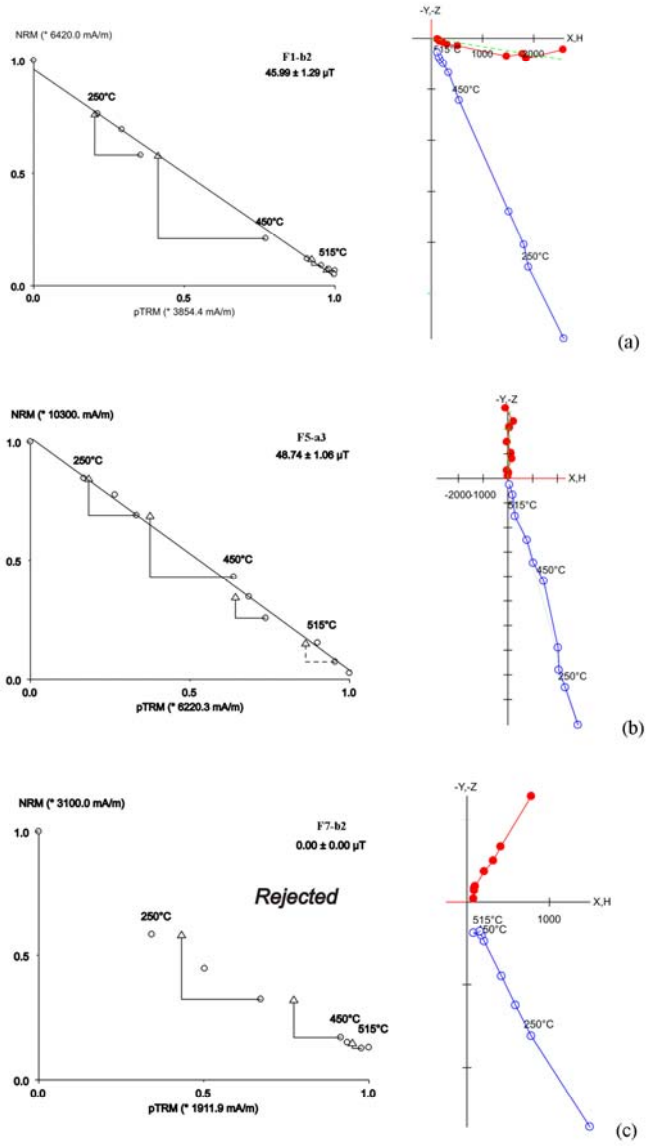
NRM (* 6420.0 mA/m)
F1-b2
45.99 ± 1.29 µT
250°C
450°C
515°C
pTRM (* 3854.4 mA/m)
-Y,-Z
X,H
1000
450°C
250°C
(a)
NRM (* 10300. mA/m)
F5-a3
48.74 ± 1.06 µT
250°C
450°C
515°C
pTRM (* 6220.3 mA/m)
-Y,-Z
X,H
-2000-1000
515°C
450°C
250°C
(b)
NRM (* 3100.0 mA/m)
F7-b2
0.00 ± 0.00 µT
Rejected
250°C
450°C
515°C
pTRM (* 1911.9 mA/m)
-Y,-Z
X,H
1000
515°C
250°C
250°C
(c)

Fig. 7

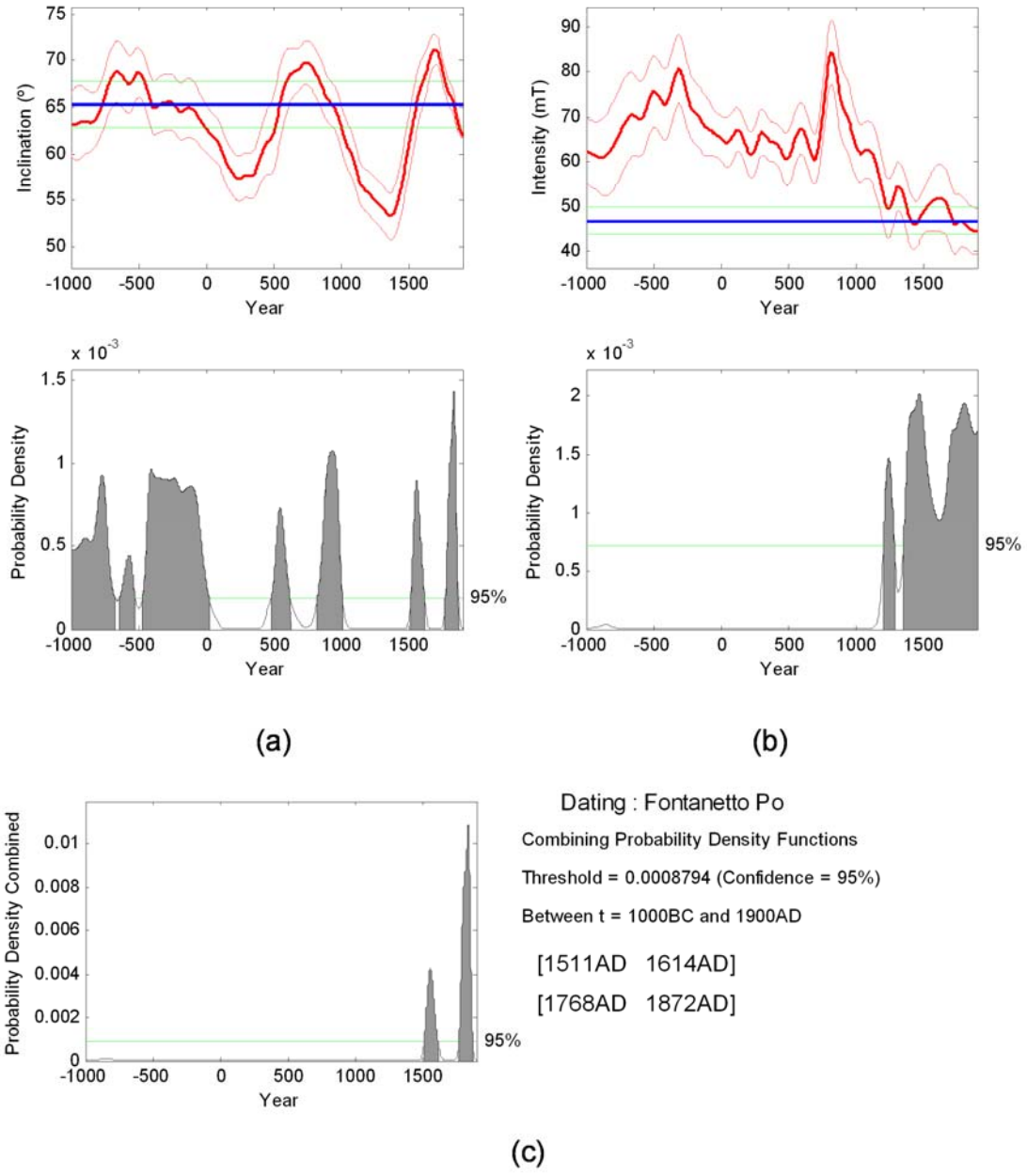
Inclination (°)
Year
Intensity (mT)
Year
x 10^-3
Probability Density
95%
Year
x 10^-3
Probability Density
95%
Year
(a)
(b)
Probability Density Combined
95%
Year
Dating : Fontanetto Po
Combining Probability Density Functions
Threshold = 0.0008794 (Confidence = 95%)
Between t = 1000BC and 1900AD
[1511AD 1614AD]
[1768AD 1872AD]
(c)

Fig. 8

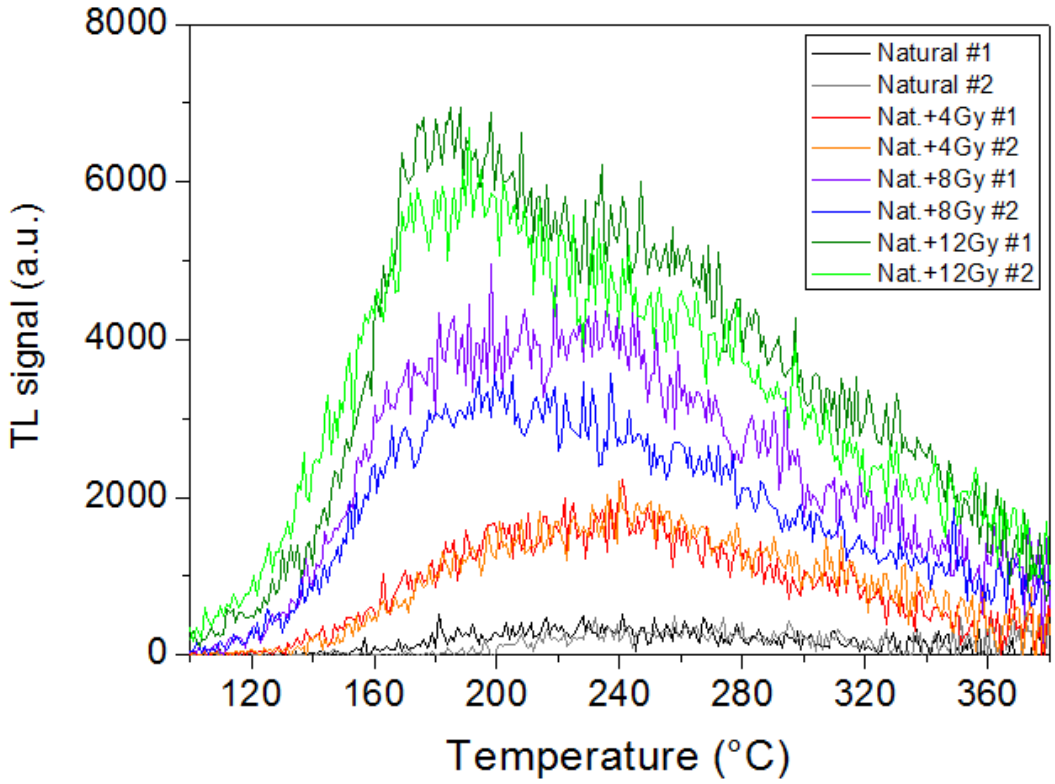
8000
6000
4000
2000
0
TL signal (a.u.)
120
160
200
240
280
320
360
Temperature (°C)
Natural #1
Natural #2
Nat.+4Gy #1
Nat.+4Gy #2
Nat.+8Gy #1
Nat.+8Gy #2
Nat.+12Gy #1
Nat.+12Gy #2

Fig. 9

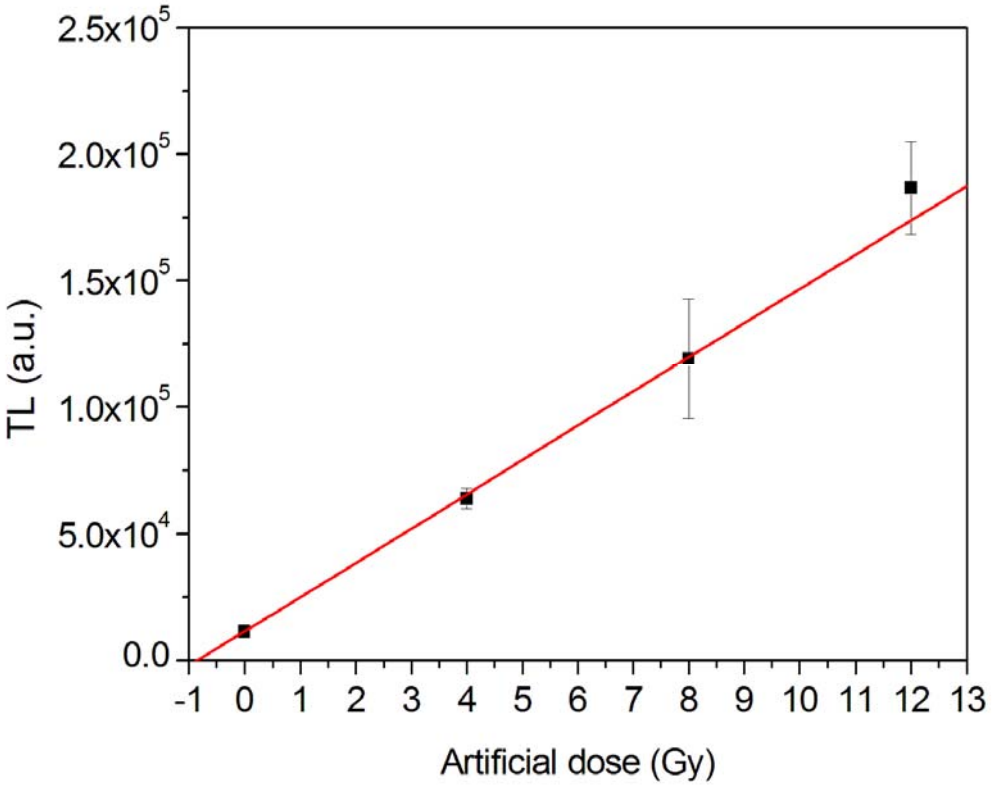
2.5x10^5
2.0x10^5
1.5x10^5
1.0x10^5
5.0x10^4
0.0
TL (a.u.)
-1 0 1 2 3 4 5 6 7 8 9 10 11 12 13
Artificial dose (Gy)

Fig. 10

Sample	Temperature range (^{o}C)	I_{ChRM} (^{o})
F1-a	80-500	69.1
F2-a1	80-500	71.6
F3-a1	80-500	67.2
F4-a	80-540	60.0
F5-a1	80-500	71.8
F6-a1	80-500	59.5
F7-a	80-540	61.4
F8-a1	80-540	66.1
F9-a	80-500	62.6
F10-a1	140-540	67.8
F11-a1	200-540	59.8
F12-a	100-540	60.2
F13-a1	80-540	63.0
F14-a2	80-540	63.9
F15-a1	80-540	68.6
F16-a1	80-540	67.9
F17-a1	200-540	69.9
F18-a1	80-540	67.6
F19-a	80-540	63.8
F20-a	80-500	68.3
F21-a1	80-540	69.8
F22-a2	80-540	55.9
F23-a1	80-500	57.5

Mean inclination

I_{CrRM}= 65.3^{o}	**α_{95} = 2.4^{o}**	**k = 156**	**N= 23**	**n= 23**

Table 1

Specimen	Paleoint (μT)	Paleoint ATRM corr	Paleoint ATRM + CR corr	σ (μT)	Tmin (°C)	Tmax (°C)	N	slope	β	f	g	q	Mad	Drat
F1-b2	46.0	45.1	43.9	1.3	20	560	10	-1.53	0.03	0.950	0.750	25.6	2.1	3.2
F1-c1	45.3	43.1	42.1	1.9	20	560	10	-1.51	0.04	0.900	0.740	16.2	1.5	4.3
F2-b2	*43.7*	*42.9*	*TRM_{1-3} > 15%*	*1.7*	*20*	*560*	*10*	*-1.46*	*0.04*	*0.980*	*0.730*	*18.9*	*1.4*	*4.0*
F3-a2	46.1	46.9	43.9	1.3	20	515	8	-1.54	0.03	0.720	0.840	22.2	2.3	1.5
F3-c1	47.0	47.3	47.3*	2.9	20	450	5	-1.57	0.06	0.890	0.690	9.9	1.5	4.1
F5-a2	48.1	47.7	43.5	1.3	20	475	6	-1.60	0.03	0.650	0.770	18.4	3.5	1.7
F5-a3	48.7	48.1	44.4	1.1	20	560	10	-1.62	0.02	0.960	0.840	37.4	2.5	2.3
F6-a2	53.6	52.1	46.6	1.3	250	475	5	-1.78	0.02	0.520	0.660	14.5	3.0	1.5
F7-b2	N/R													
F7-c1	51.2	49.9	48.6	2.7	20	350	4	-1.71	0.05	0.550	0.490	5.1	2.7	1.9
F8-a2	53.9	53.8	48.2	2.3	20	515	8	-1.80	0.04	0.880	0.750	15.8	2.9	2.5
F9-b1	50.1	50.7	44.5	0.5	20	515	8	-1.67	0.01	0.870	0.790	71.0	1.6	2.5
F9-c1	55.5	53.8	48.9	1.8	20	515	8	-1.85	0.03	0.830	0.820	20.6	3.6	3.5
F9-c2	58.3	54.6	47.4	1.7	20	560	10	-1.94	0.03	0.960	0.850	27.7	3.8	3.7
F11-b1	49.5	48.9	43.8	1.5	20	450	5	-1.65	0.03	0.520	0.670	11.7	2.3	0.6
F12-c1	48.9	48.1	44.3	0.7	20	540	9	-1.63	0.01	0.950	0.850	56.2	1.8	1.6
F12-d	45.6	50.3	47.8	1.0	20	560	10	-1.52	0.02	0.960	0.860	39.6	1.6	1.3
F16-a2	*37.8*	*36.5*	*36.5*	*2.6*	*350*	*560*	*7*	*-1.26*	*0.07*	*0.460*	*0.510*	*3.4*	*1.2*	*14.8*

F17-b1	50.6	50.9	50.9*	2.4	20	350	4	-1.69	0.05	0.630	0.610	8.0	6.4	1.4
F18-c1	52.0	51.0	51.0*	0.8	20	350	4	-1.73	0.02	0.570	0.480	17.8	1.9	0.5
F19-c1	53.5	51.9	51.1	1.9	20	350	4	-1.78	0.04	0.600	0.340	5.7	3.2	0.4
F21-a2	45.8	43.6	43.6*	3.4	20	540	9	-1.53	0.07	0.970	0.750	9.9	2.8	9.5
Site mean =	**50.0**	**49.3**	**46.4**											
Stddev =	**3.7**	**3.3**	**2.9**											

Table 2

Sample	ED (Gy)	I (Gy)	P (Gy)	Alfa counts (counts/ks)	Potassium (%)	Water (%)	k-value	Alfa Dose (mGy/year)	Beta Dose (mGy/year)	Gamma Dose (mGy/year)	Annual Dose (mGy/year)	Age (AD)
F18	0.61 ± 0.04	0.51 ± 0.05	1.12 ± 0.06	13.0 ± 0.1	0.89 ± 0.02	18 ± 1	0.29 ± 0.07	4.9 ± 1.2	1.40 ± 0.17	1.34 ± 0.35	7.6 ± 1.3	1864 ± 25
F19	0.86 ± 0.05	0.21 ± 0.07	1.07 ± 0.09	12.9 ± 0.1	0.84 ± 0.02	21 ± 1	0.24 ± 0.05	4.1 ± 1.1	1.33 ± 0.17	1.34 ± 0.35	6.8 ± 1.2	1854 ± 29

Table 3